Neurophotonics

Neurophotonics.SPIEDigitalLibrary.org

High-throughput spatial light modulation two-photon microscopy for fast functional imaging

Paolo Pozzi
Daniela Gandolfi
Marialuisa Tognolina
Giuseppe Chirico
Jonathan Mapelli
Egidio D'Angelo

SPIE.

Neurophotonics 2(1), 015005 (Jan–Mar 2015)

High-throughput spatial light modulation two-photon microscopy for fast functional imaging

Paolo Pozzi,[a,†] Daniela Gandolfi,[b,c,†] Marialuisa Tognolina,[b] Giuseppe Chirico,[a] Jonathan Mapelli,[c,*] and Egidio D'Angelo[b,d,*]
[a]University of Milan-Bicocca, Department of Physics, Piazza della Scienza 3, 20126 Milano, Italy
[b]University of Pavia, Department of Brain and Behavioural Sciences, Via Forlanini 6, 27100 Pavia, Italy
[c]University of Modena and Reggio Emilia, Department of Biomedical, Metabolic and Neural Sciences, Via Campi 287, 41125 Modena, Italy
[d]Brain Connctivity Center, Fondazione C. Mondino, Via Mondino 2, 27100 Pavia, Italy

Abstract. The optical monitoring of multiple single neuron activities requires high-throughput parallel acquisition of signals at millisecond temporal resolution. To this aim, holographic two-photon microscopy (2PM) based on spatial light modulators (SLMs) has been developed in combination with standard laser scanning microscopes. This requires complex coordinate transformations for the generation of holographic patterns illuminating the points of interest. We present a simpler and fully digital setup (SLM-2PM) which collects three-dimensional two-photon images by only exploiting the SLM. This configuration leads to an accurate placement of laser beamlets over small focal volumes, eliminating mechanically moving parts and making the system stable over long acquisition times. Fluorescence signals are diffraction limited and are acquired through a pixelated detector, setting the actual limit to the acquisition rate. High-resolution structural images were acquired by raster-scanning the sample with a regular grid of excitation focal volumes. These images allowed the selection of the structures to be further investigated through an interactive operator-guided selection process. Functional signals were collected by illuminating all the preselected points with a single hologram. This process is exemplified for high-speed (up to 1 kHz) two-photon calcium imaging on acute cerebellar slices. [DOI: 10.1117/1.NPh.2.1.015005]

Keywords: spatial light modulators; two-photon microscopy; calcium imaging; cerebellum.

Paper 14076R received Nov. 11, 2014; accepted for publication Jan. 8, 2015; published online Feb. 9, 2015.

1 Introduction

The inferior limit of the operational time scale employed by neuronal networks is determined by the duration of a single action potential (~1 ms); therefore, the ideal acquisition frequency in functional microscopy (e.g., calcium imaging or voltage-sensitive dye imaging) should be at least 1 kHz.[1] However, traditional two-photon microscopy (2PM) has a limitation in the acquisition frequency to only a few tenths of hertz due to the use of galvanometric mirrors.

Higher frame rates can be achieved by multiphoton multifocal techniques, but the highest reported frame rate over a wide field of view is 200 frames per second,[2] which is still an order of magnitude slower than neuronal activity.

A similar approach is given by temporally focused 2PM,[3] in which a single confocal plane can be simultaneously illuminated through two-photon excitation without scanning diffraction-limited volumes. However, the maximum acquisition frequency provided by this system is 30 Hz and high-speed recordings can be exclusively obtained over a small area (less than $100 \times 100\ \mu m^2$).[4]

Scanning with a random access (RA) pattern,[1,5–7] especially if performed with acousto-optic-deflectors, allows the acquisition frequencies in the kilohertz range onto multiple points of interest (POIs). However, the serial nature of this method limits the acquisition frequency when increasing the number of POIs, and kilohertz scale recordings can only be performed on few sites.

The only two-photon technique reported so far capable of simultaneously acquiring an arbitrary number of signals on the kilohertz scale is spatial light modulator (SLM) microscopy.[8] SLM microscopy takes advantage of Fourier optics to spatially modulate the coherent excitation light, thus enabling the simultaneous irradiation of an arbitrary number of POIs throughout the sample.[9] Fluorescence emission is then acquired in parallel by a pixelated detector.

The early implementations of two-photon SLM microscopes were realized by coupling a SLM to a standard laser scanning microscope. In that configuration, the image of the sample was acquired with a traditional raster scan of a single excitation volume.[6] The image was then employed to determine the POIs in which the SLM would create the excitation spots. This procedure required a complex matching of coordinates between the SLM inputs and the scanning images, prolonging calibration times, and making it difficult to precisely place the POIs on micrometer-scale structures of the sample.[10]

This paper presents a spatial light modulator-two-photon microscope (SLM-2PM) generating diffraction-limited two-photon images and acquiring neuronal signals at a high-sampling rate from multiple POIs within the focal plane with submicrometer precision. The system is scanless, as it operates without traditional galvanometric mirrors or acousto-optic deflectors. Similar approaches were adopted in linear optics confocal microscopy and applied to the generation of full-field imaging for optical manipulation.[7]

*Address all correspondence to: Jonathan Mapelli, E-mail: jonathan.mapelli@unimore.it; Egidio D'Angelo, E-mail: dangelo@unipv.it

†Authors contributed equally to this paper.

0091-3286/2015/$25.00

SLM-2PM, through its fully digital nature, gains simplicity of construction and high precision in laser beam positioning. Moreover, through appropriate software control, it can be used to generate three-dimensional (3-D) diffraction-limited images of the tissue. For demonstration purposes, SLM-2PM here is used for two-photon calcium imaging experiments,[11] improving the temporal resolution of traditional calcium imaging,[12] which is mainly limited by the serial detection of spatially separated signals.[1,5,6,13–17]

2 Materials and Methods

2.1 *Optical Setup*

The optical setup consists of a custom-made upright two-photon holographic microscope (Fig. 1). Two-photon excitation is supplied by a Ti:Sapphire laser (Chameleon Ultra II, Coherent, USA) providing 4 W maximum power at $\lambda = 800$ nm. Polarization of the laser light is set to be vertical with a Glan-Taylor polarizer, preceded by a $\lambda/2$ plate for power tuning. The laser is collimated and expanded by a 6× beam expander ($f1 = 25$ mm, $f2 = 150$ mm) and impinges at 9 deg on the reflective SLM (X10468-7, Hamamatsu), which allows an encoding phase from 0 to 2π on the beam profile with a 800×600 pixel resolution and 8-bit pixel depth. The SLM plane is conjugated through a beam reducer ($f1 = 400$ mm, $f2 = 250$ mm) to the entrance pupil of a microscope objective (Zeiss Plan-APOCHROMAT 20× 1.0 NA or Zeiss Plan-APOCHROMAT 40× 1.0 NA). The beam reducer focal lengths were chosen to fill the objective entrance pupil. In this configuration, the electric field distribution on the objective focal plane is equal to the Fourier transform of the electric field distribution on the SLM plane. Since only phases of the electric field can be encoded on the SLM, the Gerchberg–Saxon (GS) iterative algorithm[18,19] was adopted to compute the phase distribution that best reproduces the desired intensity pattern. It is important to notice that an image of the desired pattern is formed on the focal plane of the first lens of the beam reducer. A common problem in SLM-based systems is the presence of the "zeroth order" of diffraction, a fraction of the excitation light which is not shaped by the SLM. This light in turn produces a bright focal volume at the center of the field of view, inducing photodamage in the sample and generating artifacts on images. This undesired contribution can be removed with a beam blocker in the focal plane of the first lens of the beam reducer; however, this would create a dark area at the center of the field of view where no FP can be positioned. In order to remove the zeroth order of diffraction while keeping the ability to place FPs throughout the field of view, a Fresnel lens pattern was superimposed on each calculated phase mask. The image of the desired pattern after the first lens of the beam reducer is thus formed on a different plane, while the zeroth order remains focused in the lens focal plane and can be stopped by a beam blocker without affecting the pattern. The position of the second lens is slightly moved to compensate for the pattern shift and to generate an image of the desired pattern in the objective's focal plane.

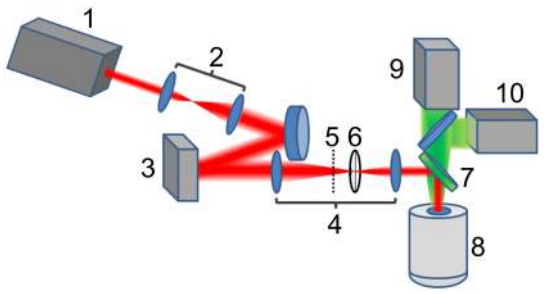

Fig. 1 Spatial light modulator-two-photon microscope (SLM-2PM) scheme: (1) Ti:Sa laser (Chameleon Ultra II, Coherent); (2) beam expander ($f1 = 2.5$ cm, $f2 = 15$ cm); (3) SLM (X10468-07, Hamamatsu); (4) beam reducer ($f3 = 40$ cm, $f4 = 25$ cm); (5) pattern formation plane; (6) copper wire for undiffracted light removal; (7) objective (Zeiss Plan-APOCHROMAT 20× 1.0 NA or Zeiss Plan-APOCHROMAT 40× 1.0 NA); (8) dichroic filter (750 nm, 750dcspxr, Chroma); (9) pixelated detector (Coolsnap, Photometrics or MicamUltima, Scimedia). (10) High speed pixelated detector (MicamUltima, Scimedia).

Fluorescence light from the sample is then collected by the objective and separated from the excitation light through a dichroic mirror (750 nm, 750dcspxr, Chroma) and a bandpass filter. An image of the objective focal plane is formed by a tube lens ($f = 125$ mm) on the detector. A flip mirror is used to create the image on one of the two pixelated sensors, a high-frequency complementary metal-oxide semiconductor (CMOS) camera (MicamUltima, Scimedia) for data acquisition or a high-resolution cooled charge-coupled device (CCD) camera (Coolsnap HQ, Photometics) for image formation. A bright-field transmission image of the sample was obtained through Köhler transillumination.

2.2 *Phase Mask Calculation*

SLM-2PM is capable of illuminating the objective focal plane in several diffraction limited points. This is achieved through a reflective phase-only SLM, a pixelated liquid crystal device shifting of an arbitrary phase the radiation reflected by each pixel. In order to illuminate the focal plane with a desired intensity pattern, the phase shift applied by every pixel of the SLM must be calculated. The matrix of phase shift values (each ranging from 0 to 2π), called the phase mask, is usually generated with slowly converging iterative algorithms.[9,18,19] For the purpose of SLM-2PM microscopy, a low number of iterations can be performed since a phase mask must be computed in a time compatible with experimental needs (seconds). Nonetheless, the phase mask must be accurate enough to guarantee that every single POI is illuminated by a diffraction-limited focal volume, as the efficiency of two-photon excitation decreases as the excitation volume increases.[13]

The classical Fourier transform-based GS algorithm[18] proved to be the fastest available algorithm capable of reliably creating diffraction-limited focal volumes. A custom developed software based on the Python Scipy libraries[20] was used for phase mask computation. After the GS algorithm, a Fresnel lens pattern is summed to the obtained phase mask in order to avoid undiffracted light illumination on the sample (see Sec. 2.1). Changing the focal power of the Fresnel lens summed to the phase mask allows the illumination of planes above and below the objective focal plane.

2.3 *Two-Photon Image Formation*

Two-photon images of the sample were obtained by computing a sequence of phase masks, each corresponding to a square grid pattern (sliding grid) of diffraction-limited (beam waist $\omega 0 = 400$ nm for 1.0 NA objective) focal points (FPs) regularly

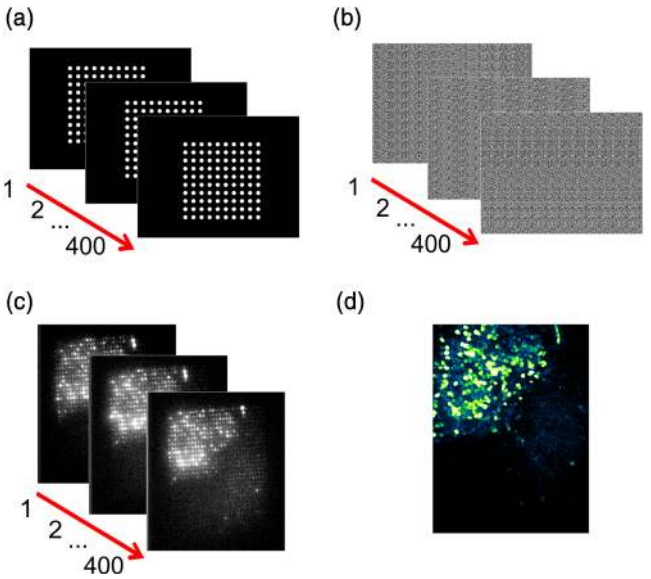

Fig. 2 Image acquisition and reconstruction: (a) A set of square grid patterns covering the entire scanning area in a raster-scan sequence is generated and (b) the corresponding holograms are computed with the Gerchberg–Saxton algorithm. The series of holograms is shown on the SLM surface, and the resulting wavefront is projected on the sample. (c) An image of the sample is acquired for every frame of the sequence, and the fluorescence of each excitation volume is stored. (d) The stored fluorescence signals are converted to grayscale values and assigned to the corresponding pixels of the reconstructed image. The numbers in (a), (b), and (c) indicate the frame index.

spaced at a distance dFP. The sequence of phase masks is calculated so that the sliding grid performs a raster scan movement in which each spot scans a small square region. The image acquisition is performed by illuminating the sample with the sequence of phase masks. The pixelated detector acquires a stream of images synchronously with the SLM refresh, so that each frame shows the two-photon fluorescence signal elicited by one phase pattern of the sequence. For every acquired frame, the fluorescence intensity of each FP is integrated and stored. The final image is obtained by assigning to each pixel the fluorescence signal of the corresponding FP (Fig. 2).

The maximum refresh rate of our SLM is limited to 60 Hz, thus making a raster scan procedure sensibly slower than using a standard galvanometric scanner. In order to limit the time for image formation, the number of frames was minimized by reducing the spatial sampling of the sliding grid motion and increasing the number of FPs per frame. A large area of the field of view of the objective ($200 \times 200\ \mu m^2$ for a 40× objective) was covered by optically oversampling the sliding grid (~ 2 pixels/$\omega 0$); 600×600 FP positions are needed. This image sampling can be achieved with a sequence of 400 phase masks, representing a sliding grid of 30×30 FPs, each moving on a 20×20 raster scan pattern. A further increase in FPs number per frame mask is not feasible, as the excitation power per FP would become too low ($\ll 1$ mW per FP) to determine detectable two-photon fluorescence. The minimum time required with this mode of image acquisition with a 60 Hz refresh rate is around 10 s. Moreover, depending on the sensitivity of the detector and on the intensity of the fluorescence signal, longer exposure times per image may be required to obtain a better signal-to-noise (S/N) ratio.

2.4 *Live Imaging*

Live imaging is needed for the selection of the plane on which measurements should be performed. To achieve two-photon live imaging, a slightly undersampled sliding grid (~ 0.75 pixels/$\omega 0$) is projected on the sample at the maximum SLM refresh frequency, while the pixelated detector acquires a single image with an exposure time equals to the entire sliding grid sequence duration. Using a sliding grid of 28×28 FPs moving in a 6×6 raster scan pattern, the result is a live stream of two-photon images at about 2 frames per second.

2.5 *Multispot Illumination*

The SLM-2PM system allows the user to select an arbitrary number of POIs chosen from the acquired image and to generate a hologram illuminating each of them with diffraction-limited FPs. In order to detect the signal of each POI, a pixelated detector must be used. For a bright two-photon dye, such as Rhodamine B in methanol, the fluorescence emission rate under 10-mW excitation power on a diffraction-limited spot (collection efficiency 1%, quantum yield = 1) is about 64,000 photons/s.[21] Such a flow can be easily detected by single-photon counting systems such as photomultipliers or single-photon avalanche diodes (SPAD). However, high-performance CCD and CMOS cameras can detect such a flow with a high S/N ratio. As the used CMOS camera has a dark noise of 400 e^- for 1 ms exposure and 65% quantum efficiency, around 20 to 30 molecules per excitation volume ($\sim 0.1\ \mu M$) are required for an S/N ratio of 2. The system is, therefore, theoretically capable of detecting signal variations at 1 kHz.

2.6 *Slices Preparation and Calcium Imaging*

Acute cerebellar slices (200-μm thick) were obtained from 18- to 25-day-old Wistar rats.[22] Rats were anesthetized with halothane (0.5 ml in 2 L for 1 to 2 min) before being killed by decapitation. All experiments were conducted in accordance with international guidelines from the European Community Council Directive 86/609/EEC on the ethical use of animals. The cerebellum was gently removed, and the vermis was isolated, fixed with cyanoacrylate glue, and immersed into a cold (2 to 3°C) cutting solution. Slices were cut in the sagittal plane. The cutting solution contained (in mM): 130 K-gluconate, 15 KCl, 0.2 EGTA, 20 HEPES, 10 glucose, pH 7.4 with NaOH. Slices were then transferred to an oxygenated Krebs' solution containing (in mM): 120 NaCl, 2 KCl, 1.2 $MgSO_4$, 26 $NaHCO_3$, 1.2 KH_2PO_4, 2 $CaCl_2$, 11 glucose, pH 7.4 when equilibrated with 95% $O_2 - 5\%CO_2$. For extracellular bulk loading, slices were deposited onto the bottom of a small Petri dish (35 mm × 10 mm) filled with 2 ml of artificial cerebrospinal fluid, and ventilated with 95% O_2/5% CO_2. A 50-μg aliquot of Fura-2AM (Molecular Probes, Eugene, Oregon) was prepared in 48 μl dimethyl sulfoxide and 2 μl Pluronic F-127 (Molecular Probes).[23] The dye aliquot was then placed on top of the slice in the Petri dish and slices were incubated in the dark at 35°C to 37°C for up to 60 min. Slices were maintained at room temperature for at least 30 min before transferring them to the recording chamber. Slices were positioned on the recording chamber and fixed with a nylon mesh attached to platinum Ω-wire to improve tissue adhesion and mechanical stability. Perfusion of oxygenated Krebs' solution at room temperature was continued during

the recording session. During acquisition, neuronal activity was elicited by mossy fiber stimulation, performed through a tungsten bipolar electrode at 20 to 30 V. Stimulation trains consist of 10 pulses of 0.2 ms duration at a frequency of 50 Hz. In order to prove that the acquired signals were in fact elicited by neuronal activity instead of artifacts created by stimulation (i.e., tissue or solution motion), the tissue was perfused with 20 μM Gabazine, a GABA-A receptor blocker, and subsequently with 50 μM APV, an NMDA receptor blocker, and 10 μM NBQX, an AMPA receptor blocker. As expected,[24,25] Gabazine perfusion leads to an increment in the number of responding granule cells (+89.1% ±11.3%; $n = 15$ slices; $p < 0.01$) and calcium signals' amplitudes (+129.9% ±2.5%; $n = 15$ slices; $p < 0.001$). Moreover, APV and NBQX perfusions completely and reversibly blocked all neuronal activities elicited by synaptic transmission.[11]

2.7 *Experimental Procedure*

The standard calcium imaging experiment was performed as follows:

- A cerebellar slice was prepared and placed in the recording chamber.
- Brightfield imaging, obtained through Köhler illumination, was used to select a region of the slice on which to perform the experiment and to position the bipolar stimulation electrode on a mossy fiber.
- "Live imaging" acquisition method was used to verify the correct staining of the slice and to select a confocal plane, at ~50 μm under the slice surface.
- A two-photon image of the selected plane was acquired.
- The user selected the POIs on the acquired image.
- The software generated a hologram illuminating the POIs.
- Laser output power was set to ~5 to 10 mW/FP.
- Calcium signals were acquired through the CMOS camera.

3 Results

3.1 *Lateral and Axial Resolutions*

The generation of a phase mask through the GS algorithm is an iterative and slowly converging process. It is, therefore, difficult to obtain a phase mask corresponding to a truly point-like illumination. However, it is not necessary to create extremely accurate phase masks, as the dimension of the FPs is physically limited by the Abbe diffraction limit. The phase mask calculation software performed 20 GS iterations to create a single phase mask. To prove that the FPs were diffraction limited, an image of fluorescent polystyrene beads immobilized in agarose gel was acquired[26] (Fig. 3). The diameter of the polystyrene beads is 100 nm, while the theoretical lateral resolution of the system with 800 nm excitation light is 400 nm. A total of 25 microbeads profiles were fitted with a Gaussian curve on the x and y image axes. The mean FWHM of the curves was 420 ± 6 nm, proving that the FPs' dimensions were diffraction limited. The axial resolution was tested with the same polystyrene microbeads sample. 3-D images were obtained with a holographic method, shifting the axial position in 0.2 μm steps by adding a Fresnel lens to the phase masks of the sliding grid. A total of 25 microbeads axial profiles were fitted with a Gaussian curve. The mean FWHM of the obtained curves was 1.15 ± 0.08 μm, proving that the system is diffraction limited on the axial direction. System resolution was slightly lower near the edges of the field of view, possibly due to the spherical aberration or the limited performance of the SLM. Fitting over 10 spheres at a distance <20 μm from the edges of the field of view resulted in a resolution of 498 ± 8 nm laterally and 1.21 ± 0.10 nm axially.

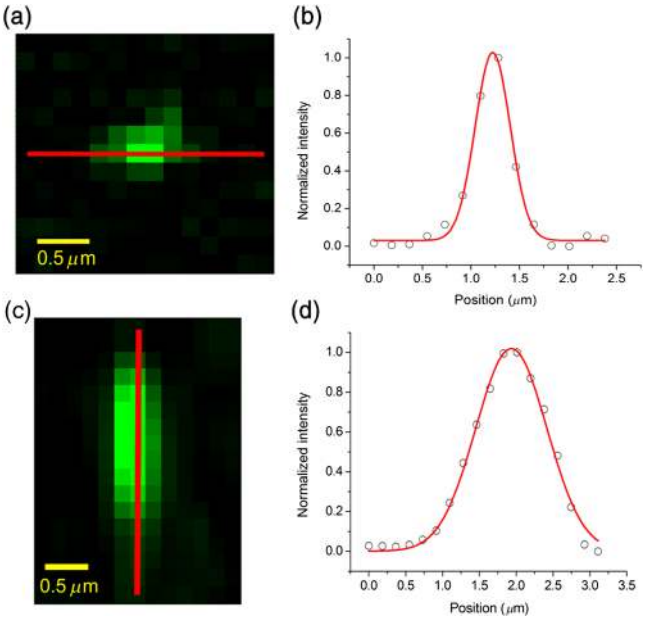

Fig. 3 Optical resolution of SLM-2PM: (a) Image of a fluorescent polistyrene bead (100-nm diameter), immobilized in 1% agarose gel. The red line indicates the section used for fitting in (b). (b) Lateral profile of a fluorescent polystyrene bead, fitted with a Gaussian function. The arrow indicates the FWHM of the curve. (c) Axial section of a three-dimensional (3-D) image of fluorescent polystyrene bead. The focal plane was shifted in 0.2 μm steps by superimposing a Fresnel lens pattern on the sliding grid phase masks. The red line indicates the section used for fitting in (d). (d) Axial profile of a single bead, fitted with a Gaussian function.

3.2 *Point of Interest Selection Precision*

The pointing accuracy of the system was assessed on a sample of under-resolved polystyrene beads with diameter 100 nm, immobilized in agarose gel. A single FP was positioned over each of 11 microbeads identified as bright spots on the full-frame acquired image. As a negative control, 11 FPs were randomly selected on the image. In response to the acquisition of a single exposure image, the FPs on the microbeads were all extremely bright. On the contrary, the randomly positioned FPs only showed a faint background fluorescence signal, proving that the POI selection accuracy is higher than half of the focal volume dimension (200 nm for 1.0 NA objectives). The confocal image of the microbeads and the multi spot illumination snapshot are shown in Fig. 4.

3.3 *Two-Photon Calcium Imaging*

The possibility to apply holographic two-photon imaging to neurobiological processes was assessed by detecting calcium signals in the granular layer of acute rat cerebellar slices. Slices

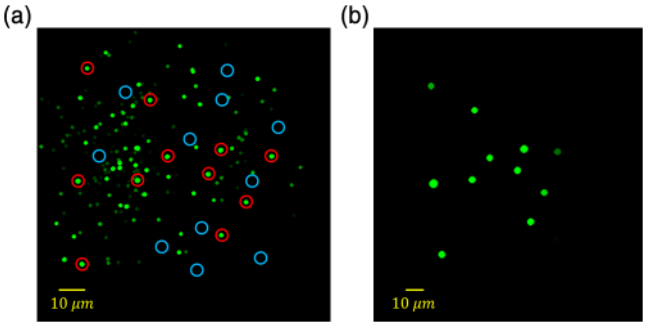

Fig. 4 Pointing precision of SLM-2PM: (a) Image (green) of fluorescent polistyrene beads (100-nm diameter, λem = 568 nm), immobilized in 1% agarose gel. Red circles indicate the selected beads for the placement of focal point (FPs). Blue circles indicate the position of control FPs placed in dark areas of the image. (b) Single exposure acquisition of the pattern illuminating the beads indicated by red circles in (a). It can be observed that only the FPs placed over fluorescent beads elicit fluorescence signal. Grayscales were manipulated in both images to enhance the contrast. Both images were processes with a maximum intensity filter (4 μm radius) in order to increase the visibility of small objects.

were bulk-loaded with cell permeant Fura-2AM (see Sec. 2). Two-photon fluorescence excitation was set at 800 nm, while fluorescence light was selected through a 515/30 bandpass filter. The Zeiss Plan-APOCHROMAT 20× 1.0 NA objective was used, leading to a camera field of view of about 400×400 μm^2.

Live imaging acquisition mode was used for confocal plane selection which was typically 50 to 60 μm deep in the cerebellar slice. A standard two-photon image of the selected plane was acquired with a 400 frames 30×30 FPs scanning grid, covering a rectangular area of 220×300 μm^2. Laser power was set to 4 mW/FP. CCD camera and SLM refresh rate were set to 50 ms per frame in order to obtain an image with a high S/N ratio, for a total image acquisition time of 20 s. The POIs were selected within the soma of each visible granule cell. During signal acquisition, laser power was set to ~10 mW per FP. Calcium transients were recorded by the high-speed CMOS camera at frequencies up to 1 kHz. Granule cells showed calcium signals variations in the order of 5% to 10% ($\Delta F/F_0$) peaking around 100 ms after stimulation and showing an S/N ratio of around 10 at 1 kHz (Fig. 5).[11]

3.4 *Three-Dimensional Imaging*

The SLM-2PM enabled the shifting of the focal plane in the axial direction only through SLM programming, without changing the objective position. This feature can be useful for experiments requiring high-mechanical stability (i.e., patch clamp recordings). The maximum possible shift was limited by the fact that the acquisition focus remained on a fixed plane, while the excitation pattern was digitally moved. The available axial range, with a 1.0 NA objective, was limited to about 20 μm.

Figure 6 shows a Purkinje cell in an acute cerebellar slice, intracellularly loaded with Alexa488 sodium salt. The image was acquired by (1) sequentially shifting the excitation plane in 10 steps of 2 μm; (2) exciting at 750 nm with a laser power of 4 mW/FP; (3) using the Zeiss Plan-APOCHROMAT 20× 1.0 NA objective; (4) selecting fluorescence light with a 515/30 bandpass filter; (5) acquiring each confocal image with a 400 frame 30×30 FPs scanning grid, covering a rectangular area of 220×300 μm^2; and (6) acquiring each frame with a 20 ms

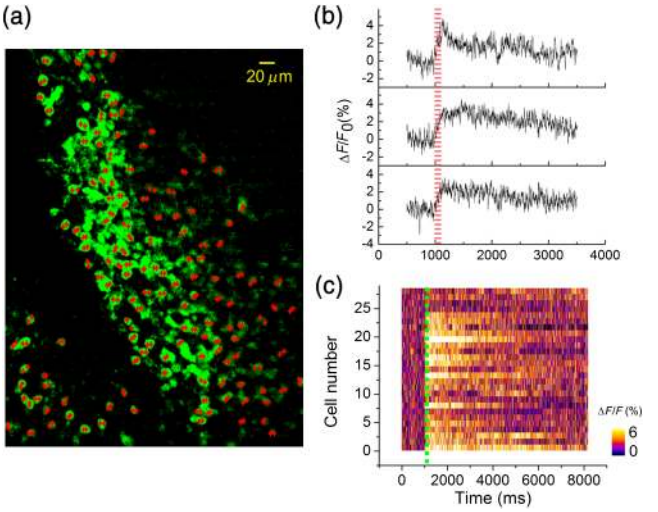

Fig. 5 High-frequency acquisition of calcium signals from multiple neurons in cerebellar slices: (a) Reconstructed image of the granular layer in an acute cerebellar slice bulk-loaded with Fura-2AM. Red crosses indicate the user selected positions for high-frequency signals acquisition. (b) Example of three different traces acquired at 1 kHz sampling rate, showing different kinetics, otherwise impossible to be discrimated at low-time resolution. The red line indicates stimulation onset. (c) Ensemble response of all 27 active cells in the sample, nonresponding granule cells are not shown. The green line indicates stimulation onset.

exposure of the camera (total acquisition time around 10 s for each confocal plane.). The same procedure was performed with the Zeiss Plan-APOCHROMAT 40× 1.0 NA objective on a single dendritic arborization to increase spatial sampling [see Fig. 6 (c)] enabling the visualization of single dendritic spines.

4 Discussion

In this paper, we present a novel multiphoton microscope, called SLM-2PM, which is based on the combination of an SLM with a pixelated detector, capable of acquiring diffraction-limited

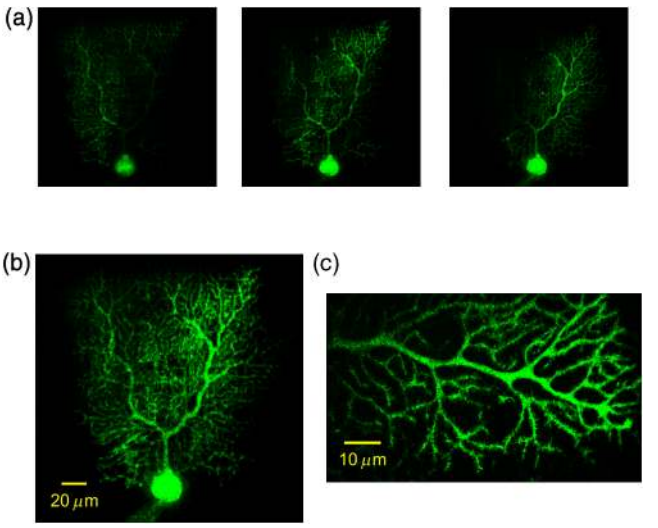

Fig. 6 3-D image of a Purkinje cell, intracellularly loaded with Alexa488. (a) Three confocal images acquired at planes 4-μm apart. (b) Overlay of 10 different confocal images showing the entire Purkinje cell. (c) Overlay of 10 different confocal images (2 μm step; 40× magnification) of a dendritic arborization in which dendritic spines are visible.

3-D two-photon images. This setup, without any mechanically moving parts, allowed the generation of illumination patterns impinging, with submicrometer precision, onto arbitrarily selected points, with the purpose of simultaneously acquiring multiple signals with kilohetrz resolution.[11]

SLM microscopy was applied to linear optics confocal imaging, and the SLM capability was exploited to generate wide field images and to selectively illuminate arbitrary POIs.[7] More recently, SLM microscopy was combined with traditional laser scanning two-photon imaging[8,27] to implement a hybrid galvos-SLM microscope. In our system, the SLM enabled the implementation of an innovative digital parallel laser scanning 2PM. This latter is implemented without moving parts and with fewer optical components than conventional 2PMs (galvanometric mirrors[13] or acousto-optic deflectors[1,6,7] coupled with photomultiplier tubes or photodiodes). Our system proved to be diffraction limited both in the axial and in the lateral directions, thus demonstrating an image generation efficiency comparable to conventional 2PMs.[28] A critical issue in experimental neuroscience is the detection of neuronal activity at deep focal planes without damaging the sample, especially when performing *in vivo* recordings. This limitation is typically overcome by employing conventional 2PMs enabling the collection of full-field images as well as functional signals deep in the tissue (below 500 μm). The SLM-2PM can achieve a high-excitation depth and low photodamage as in conventional two-photon fluorescence microscopy. However, in strongly scattering materials, the use of pixelated detectors limits the imaging efficiency, as reported in other holographic systems.[8] The fluorescence emission at deep focal planes coming from a single FP can spread over more than one pixel, thus potentially limiting the achievable imaging depth in comparison with a standard 2PM. Nevertheless, when a single pixel of the detector is used to collect light from a single FP, the camera pixel acts exactly as the confocal pinhole of a standard confocal microscope. Therefore, the acquisition depth achievable by SLM-2PM will always be higher than that of a standard, single photon, confocal microscope, due to the deeper excitation achievable. It should also be noted that the collection of signals from superficial layers is equally critical to understand neural circuit functions. In several cases, neuronal network connections spread over the horizontal planes and neuronal somata or dendritic branches are located in the upper layers. Moreover, in order to combine SLM-2PM recordings with electrophysiological methods (e.g., patch clamp), brain slice preparations offer the ideal workbench for high-throughput multitechnique recordings.

In this work, we have applied the SLM-2PM to neuroscience for the detection of fast calcium signals in rat cerebellar slices bulk stained with Fura-2AM (see Sec. 2), a calcium dye which stains the cytoplasmic compartments. It should be noted that the bulk staining procedure could prevent the generation of images from deep focal planes because of a low penetration of dye molecules. Moreover, the accumulation of dye molecules in the extracellular space might contaminate signals generated by neuronal soma (see Fig. 7). Finally, the cerebellum granular layer cells are tightly packed, and in most cases, adjacent membranes are separated by only few nanometers, making difficult to properly discriminate adjacent cells.[6,29] Nevertheless, the SLM-2PM proved capable of generating full-field images at a 50-μm depth with single-cell resolution and allowed the visualization of single isolated green fluorescent protein (GFP) positive cells at >100 μm depth (see Fig. 7), indicating that the actual

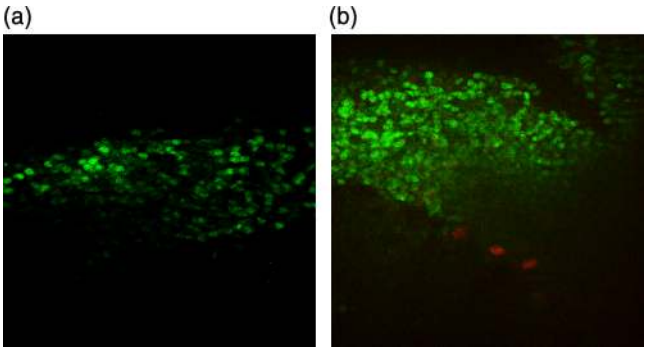

Fig. 7 Two images of the same cerebellar slice, green channel is Fura-2AM (Exc. 800 nm, Em. 515 nm), staining granule cells, red channel is EGFP (Exc. 930 nm, Em. 510 nm), expressed by inhibitory cells. (a) Image acquired near the surface of the slice (~30 to 40 μm). (b) Image acquired 50 μm below. It is important to notice how the signal from Fura-2AM is difficult to detect in depth in the sample, while the EGFP cells are easily imaged, thus proving that the main limit in imaging depth for Fura-2 calcium imaging is given by the low penetration of the dye in the tissue, and not by the optical performances of the microscope.

limitations in the SLM-2PM efficiency were not dependent on the optical apparatus, but on the sample staining. A possible solution to further increase the penetration depth (>100 μm) of the system could derive from the following modifications: (1) Reduction of the number of points in the sliding grid to increase the laser intensity per beamlet thus improving the S/N ratio; (2) increase the distance between adjacent points in the sliding grid to reduce the contamination of neighboring FPs; and (3) increase the detector sensitivity by employing an EM-CCD camera or an sCMOS camera.

We have shown that the SLM-2PM has the potential to go beyond the performances of conventional 2PMs in the acquisition of multiple fast signals. Galvanometric two-photon laser scanning microscopes are limited in providing high-acquisition rate over multiple sites.[30] Two-photon laser scanning microscopes based on acousto-optic deflector (AOD) and RA schemes[1] allow the investigation of multiple POIs, however, the use of a single laser beam limits the number of collected neurons. The number of illumination points is determined by the integration time needed to detect a significant fluorescent signal in a single position. The SLM-2PM thus has the advantage of increasing both the acquisition rate and the exposure time, which could be useful in the case of poorly emitting samples.

Furthermore, by simultaneously positioning multiple low-intensity laser beamlets, the SLM-2PM enables long-term recordings with reduced photobleaching. Although in some recordings the total laser power impinging onto neuronal tissue was above 1 W, the quadratic dependence of two-photon absorption should be carefully taken into account. When the excitation power is spread over N diffraction limited FPs, the total absorbed energy is proportional to $1/N$, which means that our setup is roughly comparable with conventional laser scanning systems with regard to applied power and potential photodamage. In order to verify this assumption, sample viability was assessed by performing long-term recordings in which calcium signals elicited by stimulation protocol remained stable for long periods (up to 3 h, see Ref. 9). Finally, it was recently shown that, by arranging a set of AODs, it is possible to obtain the 3-D scanning of a thick sample without changing the objective position.[7,16,29] The SLM-2PM proved to be efficient in acquiring

3-D diffraction limited confocal images by just shifting the excitation pattern through the SLM. In our condition (1.0 NA objective), the axial range is limited to about 20 μm. However, by using the SLM to compensate for objective aberrations on out-of-focus planes,[31] and employing an adaptive lens,[32] an axial range in the order of 100 μm could be achieved.

These observations indicate that the SLM-2PM is a versatile and promising microscope particularly suitable for neurobiological applications, to be combined with electrophysiological methods such as patch clamp recordings[11] or other cutting edge imaging techniques (e.g., optogenetic,[33] selective photostimulation,[27] fluorescence correlation spectroscopy,[34] and optical tweezing[9]). A further potential application of the SLM-2PM is voltage-sensitive dye imaging, which requires a high-sampling frequency and a high-sensitivity detector.[35] The use of new voltage-sensitive probes in combination with high-performance detectors could enable the simultaneous acquisition of action potentials in multiple single neurons.

Acknowledgments

We thank E. Hasani, A. Tomaselli, I. Cristiani, and D. Rebuzzi for participating in the initial phase of SLM-2PM implementation, G. Ferrari for excellent assistance in the setup implementation, and M. Rossin for technical support. This work was supported by European Union Grants [REALNET FP7-ICT270434, CEREBNET FP7-ITN238686, Human Brain Project (HBP-604102)] and the Italian Ministry of Health (RF-2008-INM-1143418 and RF-2009- 1475845) to Egidio D'Angelo.

References

1. R. Salome et al., "Ultrafast random-access scanning in two-photon microscopy using acousto-optic deflectors," *J. Neurosci. Methods* **154**(1–2), 161–174 (2006).
2. J. Bewersdorf, R. Pick, and S. W. Hell, "Multifocal multiphoton microscopy," *Opt. Lett.* **23**(9), 655–657 (1998).
3. D. Oron, E. Tal, and Y. Silberberg, "Scanningless depth-resolved microscopy," *Opt. Express* **13**(5), 1468–1476 (2005).
4. O. D. Therrien et al., "Wide-field multiphoton imaging of cellular dynamics in thick tissue by temporal focusing and patterned illumination," *Biomed. Opt. Express* **2**(3), 696–704 (2011).
5. G. D. Reddy et al., "Three-dimensional random access multiphoton microscopy for functional imaging of neuronal activity," *Nat. Neurosci.* **11**(6), 713–720 (2008).
6. L. Sacconi et al., "Optical recording of electrical activity in intact neuronal networks with random access second-harmonic generation microscopy," *Opt. Express* **16**(19), 14910–14921 (2008).
7. G. Katona et al., "Fast two-photon in vivo imaging with three-dimensional random-access scanning in large tissue volumes," *Nat. Methods* **9**(2), 201–208 (2012).
8. V. Nikolenko et al., "SLM microscopy: scanless two-photon imaging and photostimulation with spatial light modulators," *Front. Neural Circuits* **2**, 5 (2008).
9. J. E. Curtis, B. A. Koss, and D. G. Grier, "Dynamic holographic optical tweezers," *Opt. Commun.* **207**(1–6), 169–175 (2002).
10. S. Quirin et al., "Simultaneous imaging of neural activity in three dimensions," *Front. Neural Circuits* **8**, 29 (2014).
11. D. Gandolfi et al., "The spatiotemporal organization of cerebellar network activity resolved by two-photon imaging of multiple single neurons," *Front. Cell Neurosci.* **8**, 92 (2014).
12. O. Garaschuk et al., "Large-scale oscillatory calcium waves in the immature cortex," *Nat. Neurosci.* **3**(5), 452–459 (2000).
13. W. Denk, J. H. Strickler, and W. W. Webb, "Two-photon laser scanning fluorescence microscopy," *Science* **248**(4951), 73–76 (1990).
14. D. A. Dombeck et al., "Functional imaging of hippocampal place cells at cellular resolution during virtual navigation," *Nat. Neurosci.* **13**(11), 1433–1440 (2010).
15. P. A. Kirkby, K. M. S. Nadella, and R. A. Silver, "A compact acousto-optic lens for 2D and 3D femtosecond based 2-photon microscopy," *Opt. Express* **18**(13), 13721–13745 (2010).
16. Y. Otsu et al., "Optical monitoring of neuronal activity at high frame rate with a digital random-access multiphoton (RAMP) microscope," *J. Neurosci. Methods* **173**(2), 259–270 (2008).
17. D. S. Peterka, H. Takahashi, and R. Yuste, "Imaging voltage in neurons," *Neuron* **69**(1), 9–21 (2011).
18. R. W. Gerchberg, "A practical algorithm for the determination of phase from image and diffraction plane pictures," *Optik* **35**, 237–246 (1972).
19. C. Maurer et al., "What spatial light modulators can do for optical microscopy," *Laser Photonics Rev.* **5**(1), 81–101 (2011).
20. T. E. Oliphant, "Python for scientific computing," *Comput. Sci. Eng.* **9**(3), 10–20 (2007).
21. C. Xu and W. W. Webb, "Measurement of two-photon excitation cross sections of molecular fluorophores with data from 690 to 1050 nm," *J. Opt. Soc. Am. B* **13**(3), 481 (1996).
22. E. D'Angelo et al., "Synaptic excitation of individual rat cerebellar granule cells in situ: evidence for the role of NMDA receptors," *J. Physiol.* **484**(2), 397–413 (1995).
23. S. Kirischuk and A. Verkhratsky, "[Ca2+]i recordings from neural cells in acutely isolated cerebellar slices employing differential loading of the membrane-permeant form of the calcium indicator fura-2," *Pflugers Arch.* **431**(6), 977–983 (1996).
24. J. Mapelli, D. Gandolfi, and E. D'Angelo, "Combinatorial responses controlled by synaptic inhibition in the cerebellum granular layer," *J. Neurophysiol.* **103**(1), 250–261 (2010).
25. J. Mapelli, D. Gandolfi, and E. D'Angelo, "High-pass filtering and dynamic gain regulation enhance vertical bursts transmission along the mossy fiber pathway of cerebellum," *Front. Cell Neurosci.* **4**, 14 (2010).
26. P. Shaw and D. Rawlins, "The point-spread function of a confocal microscope—its measurement and use in deconvolution of 3-D data," *J. Microsc.* **163**, 151–165 (1991).
27. C. Lutz et al., "Holographic photolysis of caged neurotransmitters," *Nat. Methods* **5**(9), 821–827 (2008).
28. K. Svoboda et al., "In vivo dendritic calcium dynamics in neocortical pyramidal neurons," *Nature* **385**(6612), 161–165 (1997).
29. T. Fernandez-Alfonso et al., "Monitoring synaptic and neuronal activity in 3D with synthetic and genetic indicators using a compact acousto-optic lens two-photon microscope," *J. Neurosci. Methods* **222**, 69–81 (2014).
30. M. Scanziani and M. Hausser, "Electrophysiology in the age of light," *Nature* **461**(7266), 930–939 (2009).
31. K. D. Wulff et al., "Aberration correction in holographic optical tweezers," *Opt. Express* **14**(9), 4170–4175 (2006).
32. D.-Y. Zhang et al., "Fluidic adaptive lens with high focal length tunability," *Appl. Phys. Lett.* **82**(19), 3171 (2003).
33. E. Papagiakoumou et al., "Scanless two-photon excitation of channelrhodopsin-2," *Nat. Methods* **7**(10), 848–854 (2010).
34. R. A. Colyer et al., "High-throughput FCS using an LCOS spatial light modulator and an 8 × 1 SPAD array," *Biomed. Opt. Express* **1**(5), 1408–1431 (2010).
35. P. Yan et al., "Palette of fluorinated voltage-sensitive hemicyanine dyes," *Proc. Natl. Acad. Sci. U. S. A.* **109**(50), 20443–20448 (2012).

Paolo Pozzi is a postdoctoral researcher at Delft Center for System Control, in the TU Delft University. His main scientific interest is in the development of innovative fluorescence microscopy applications, with a particular interest in the exploitation of wavefront manipulation techniques.

Daniela Gandolfi holds a degree in physics and a PhD in neuroscience. She is a post-doc in the neurophysiology laboratory of the University of Pavia and her main scientific interest is the development of nonlinear imaging methods for the detection of functional signals from neuronal networks.

Marialuisa Tognolina completed her master's degree in physics at the University of Milano Bicocca in March 2013. She is currently

pursuing her PhD research in biomedical science at the University of Pavia, Italy. Her PhD research is related to the study of cerebellar network activity through spatial light modulation—two photon microscopy.

Giuseppe Chirico received his PhD in physics in 1990 from the Università degli Studi di Milano and is currently a professor of applied physics at Università degli studi di Milano-Bicocca. His interests are in optical microscopy and correlative spectroscopy for biophysics.

Jonathan Mapelli is assistant professor of physiology at the University of Modena and Reggio Emilia and co-advisor of the cellular imaging division at the Brain Connectivity Center (Pavia). His main interests in the field of optics are related to the development of linear and nonlinear imaging methods to monitor neuronal network activity and synaptic plasticity.

Egidio D'Angelo is professor of phsyiology in the Department of Brain and Behavioral Sciences, University of Pavia. He is director of the Brain Connectivity Center and of the PhD in Biomedical Sciences. His research activity concerns the functional mechanisms of cerebellar cortex microcircuits (http://www-5.unipv.it/dangelo/) using innovative electrophysiological and imaging techniques and mathematical models, integrating spiking networks into closed-loop robotic simulations and testing large-scale brain network using MRI and TMS techniques in humans in vivo.